THE ESCAPE OF PARTICLES FROM A CONFINING POTENTIAL WELL

JAMES P. LAVINE*, EDMUND K. BANGHART*, and JOSEPH M. PIMBLEY**
*Microelectronics Technology Division, Eastman Kodak Company, Rochester, NY 14650-2008
**Department of Mathematical Sciences, Renssalaer Polytechnic Institute, Troy, NY 12180-3590

ABSTRACT

Many electron devices and chemical reactions depend on the escape rate of particles confined by potential wells. When the diffusion coefficient of the particle is small, the carrier continuity or the Smoluchowski equation is used to study the escape rate. This equation includes diffusion and field-aided drift. In this work solutions to the Smoluchowski equation are probed to show how the escape rate depends on the potential well shape and well depth. It is found that the escape rate varies by up to two orders of magnitude when the potential shape differs for a fixed well depth.

1. INTRODUCTION

Interest continues to focus on the escape rate of particles from a potential well. Kramers [1] established that the escape rate depends in an exponential fashion on the well depth and that increases in the well depth lead to decreases in the escape rate. He also showed that the potential well shape enters to first-order through the well curvature at the well bottom and at the well top. The well depth, or alternatively the barrier height of the potential well, affects the operation of electron devices such as charge-coupled devices [2] or quantum-well devices [3] and the rate of chemical reactions [4-6]. When the diffusion coefficient of the particle trapped in the well is small, the carrier continuity equation, i.e., the Smoluchowski equation, is used to study the escape rate [7]. This equation includes diffusion and field-aided drift with the field the negative derivative of the potential well. Solutions to the Smoluchowski equation are probed here to learn how the escape rate depends on the potential well shape and well depth.

Several techniques lead to the dominant time dependence of the solutions of the Smoluchowski equation, that is, the τ in $e^{-t/\tau}$ with t the time [2]. Two of these approaches, eigenvalue determination and mean first passage time evaluation [4-6], are described in the next two sections. Numerical solution, closed-form expressions, and random walks are also utilized. Linear, rectangular, and polynomial potentials are investigated. All of these techniques are used in Section 4, where it is shown that τ varies by up to two orders of magnitude when the potential well shape differs for a fixed barrier height. In addition, the variation is found to grow with the barrier height. Section 5 is a summary of the present findings.

2. THE SMOLUCHOWSKI EQUATION AND ITS EIGENVALUES

Diffusion with field-aided drift is described by the Smoluchowski equation

$$\frac{\partial n(x,t)}{\partial t} = \frac{\partial}{\partial x}\left[D(x) \frac{\partial n(x,t)}{\partial x} + \frac{D(x)}{kT} q\, n(x,t) \frac{\partial W(x)}{\partial x} \right] . \qquad (1)$$

Here n(x,t) is the particle density as a function of the spatial variable x and the time t, and D(x) is the diffusion coefficient of the particle. kT/q is the thermal voltage, W(x) is the potential well, and V = qW/kT is the dimensionless potential well. When chemical reactions are considered, then x is a reaction or configuration coordinate. The model space is from x =

Mat. Res. Soc. Symp. Proc. Vol. 290. ©1993 Materials Research Society

0 to x = L. The calculations presented below use D = 12.929 cm^2/s and L = 1 μm. This D is appropriate for electrons in moderately doped silicon. The boundary conditions are reflection or zero flux at x = 0,

$$D(x)\,\frac{\partial n(x,t)}{\partial x} + \frac{D(x)}{kT}\,q\,n(x,t)\,\frac{\partial W(x)}{\partial x} = 0 \quad , \tag{2}$$

and a sink at x = L,

$$n(L,t) = 0 \quad . \tag{3}$$

Equation (1) can be solved by numerical methods [8] or by using a one-dimensional version of a random walk technique for diffusion problems [9]. However, escape problems generally require only the leading time dependence of the solutions of Eq. (1). Several approaches yield this dependence and are explored in this work.

The first approach, separation of variables, leads to

$$n(x,t) = \Sigma_n\, f_n(x)\; e^{-(t/\tau_n)} \quad , \tag{4}$$

with the sum over the eigenvalues τ_n. These are determined from the differential equation for $f_n(x)$, which is transformed into a standard Sturm-Liouville eigenvalue problem. The largest τ_n , τ_1, dominates Eq. (4), and it is found numerically with the aid of an eigenvalue determination subroutine [10]. (The second eigenvalue is found to be smaller by a factor of 50 or more for the present case.) Figure 1 shows a potential well that is defined with two parabolas and was used by Hong and Noolandi in their study of surface desorption [11]. The parabolas are matched at $x = x_B$, which for Fig. 1 is 0.5 L. The dependence of τ_1 on the barrier height, or equivalently the well depth, is presented in Fig. 2. The exponential dependence on barrier height predicted by Kramers [1] is evident as the barrier height increases.

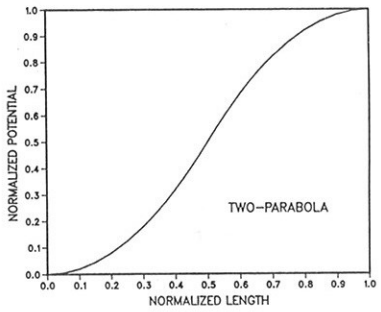

Fig. 1. Normalized potential vs normalized length for the two-parabola potential well.

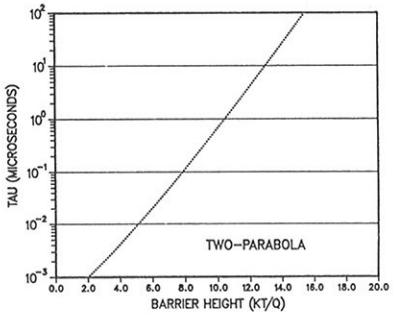

Fig. 2. Dominant eigenvalue τ_1 vs barrier height for the two-parabola potential well.

3. MEAN FIRST PASSAGE TIME

The dominant time dependence of the solutions of Eq. (1) is also found through the calculation of the mean first passage time τ. This approach is reviewed by Hänggi et al. [6] and is well-covered in the mathematical and mathematical physics literature [4,5,12-14]. The present derivation follows Weaver [15-16] and Deutch [17].

The particles escape the potential well at x = L where the flux is proportional to $\partial n(L,t)/\partial x$, (by Eq. (3), n(L,t) = 0). Thus,

$$\tau(\varepsilon) = \int_0^\infty dt\; t\; \partial n(L,t)/\partial x \;/\; \int_0^\infty dt\; \partial n(L,t)/\partial x \quad , \tag{5}$$

with $n(x,t = 0) = \delta(x - \varepsilon)$, the initial condition for the particle distribution. Equation (5) is evaluated through the use of the Laplace transform technique on Eqs. (1), (2), and (3). The result is

$$\tau(\varepsilon) = \int_\varepsilon^L dy\, D^{-1}(y)\, e^{V(y)} \int_0^y dz\, e^{-V(z)} \quad . \tag{6}$$

This double integral can be evaluated numerically or in closed form for simple potential well shapes [15]. $\tau(\varepsilon)$ is related to a sum over the eigenvalues of Section 2 [18]. $\tau(\varepsilon)$ exceeds τ_1 and when the first eigenvalue is dominant, then $\tau(\varepsilon) \sim \tau_1$. Selected numerical results with Eq. (6) are presented in this and the next section.

The mean first passage times $\tau(\varepsilon)$ for the two-parabola potential agree with the eigenvalue results to better than 3% for barrier heights of a few kT/q. The $\tau(\varepsilon)$ is always greater than the eigenvalue as expected [18], and the eigenvalue τ_1 quickly approaches $\tau(\varepsilon)$ as the barrier height increases. Figure 3 shows how $\tau(\varepsilon)$ depends on the location of the matching point, x_B, of the two parabolas. The potential at x_B is set to half of the barrier height and the initial particle density is at ε = 0.1 L. It is seen that $\tau(\varepsilon)$ decreases and, hence, the escape rate increases with an increase in x_B. The spread in the results is about a factor of 5 to 6, and is approximately equal to the change in the product of the potential well curvatures at x = 0 and x = L, which is 5.6. This is based on the prefactor of Kramers'

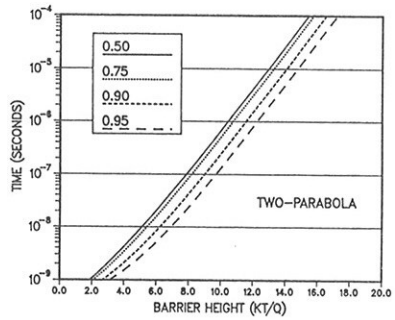

Fig. 3. Mean first passage time vs barrier height for the two-parabola potential well when the location of the half-height point (in μm) varies.

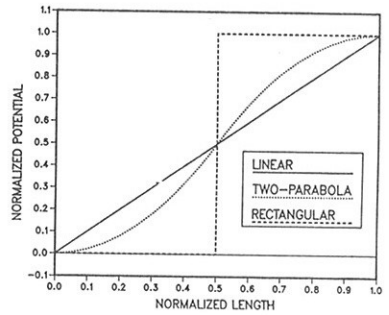

Fig. 4. Normalized potential vs normalized length for linear, two-parabola, and rectangular potential wells.

escape rate [1], which is given in Eq. (17) of Ref. [1] and Eq. (19) of Hong and Noolandi [11]. The numerical results also show a symmetry, i.e., the $\tau(\varepsilon)$ for $x_B = 0.5\ L - d$ equals that for $x_B = 0.5\ L + d$. This also follows from an examination of the product of curvatures when $V(x_B)$ equals half the barrier height.

4. WELL SHAPE EFFECTS

The previous sections described two numerical techniques for the determination of the leading time dependence for particle escape from a potential well. This section compares the τ for several well shapes. Figure 4 compares a linear, a two-parabola, and a rectangular potential well. The $\tau(\varepsilon)$ for the linear potential comes from Eq. (6) and for $\varepsilon = 0$ is

$$\tau = \{L^2/(V\ D)\}\ [\{(e^V - 1)/V\} - 1] \quad . \qquad (7)$$

Here V is the barrier height in units of kT/q. Random walk results agree with those from Eq. (7) and with those from the numerical integration of Section 3 for the linear potential. The eigenvalue approach of Section 2 provides the τ for the two-parabola case with $x_B = 0.5$ L. The τ for the rectangular barrier is obtained from an approximation to the eigenvalue expression developed [2,19] from Eq. (1),

$$\tau = \{\ \alpha\ (1-\alpha)L^2/\ D\ \}\ e^V \quad , \qquad (8)$$

with x_B the start of the rectangular barrier, $\alpha = x_B/L$, and V the barrier height in units of kT/q.

The τ for the potentials of Fig. 4 are compared in Fig. 5. The spread in τ quickly approaches a factor of ten for barrier heights of about 6 kT/q. The spread continues to increase with increases in the barrier height and approaches a factor of 100. The results for the rectangular potential deviate significantly from the other two shapes, although the two-parabola results are a factor of 5 or so above the linear potential results. The rectangular potential includes a field-free drift region from $x = x_B = 0.5$ L to the sink at x = L. This region increases τ significantly, as is made clear in Fig. 6. Here τ is plotted for a field-free drift region of 0.1, 0.3, and 0.5 μm with the last case from Fig. 5. The value of τ decreases with the decrease in the extent of the field-free drift region and approaches the results for the two-parabola case. Thus, attention must be paid to the part of the potential well between the maximum in the potential and the location of the sink.

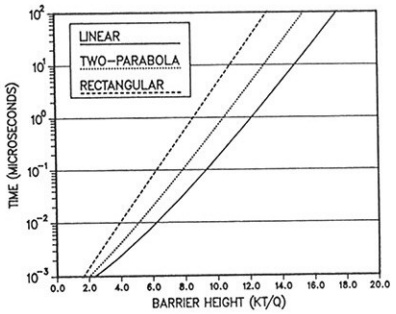

Fig. 5. τ vs barrier height for the potential wells of Fig. 4.

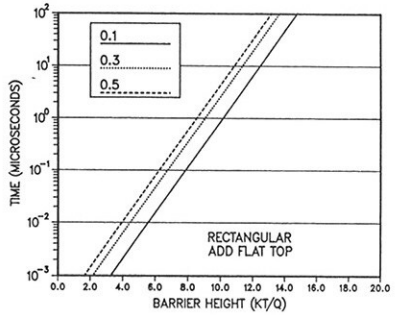

Fig. 6. τ vs barrier height for the rectangular potential with a 0.5 μm well. The length (in μm) of the top field-free region varies.

This finding is emphasized by the final set of results. These are for the two-parabola potential well with a third parabola matched at x = 1.0 μm. The sink is now where the added parabolic potential goes to zero, so that the model space is extended. The increases in τ are shown in Figs. 7 and 8, where the added parabola is convex and concave, respectively. It is noteworthy that the increase is less for the same added length when the added section is concave.

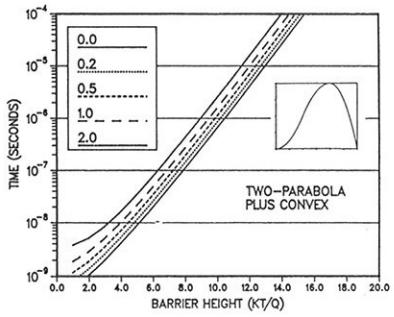

Fig. 7. τ vs barrier height for the two-parabola plus convex region of varying length in μm. The insert is the potential well shape.

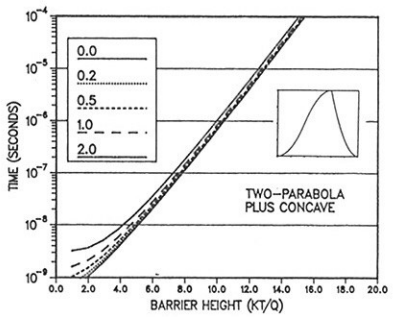

Fig. 8. τ vs barrier height for the two-parabola plus concave region of varying length in μm. The insert is the potential well shape.

5. SUMMARY

This work has presented several techniques for determining the escape rate of a particle from a potential well, when the particle motion is described by the Smoluchowski equation. The results may be scaled for changes in the length of the model space and in the value of the diffusion coefficient. The numerical results show that the barrier height dominates the value of the escape rate, but that the shape of the potential well also has a strong effect on the escape rate. The τ values are spread by a factor of 5 to almost a factor of 100 when the potential well shape is varied for a fixed barrier height. In addition, τ is affected by the shape of the potential well before the sink location, but past the potential maximum. The effects of increases in τ are amplified in the escape rate, because of the exponential time dependence of the particle density on τ. These surprising findings mean that increased attention must be paid to the potential well shape in escape problems.

ACKNOWLEDGEMENTS

We thank Professor David L. Weaver for informative and helpful discussions and a series of references. We also thank Drs. Peter E. Castro and David S. Ross for their assistance.

References

1. H.A. Kramers, Physica **7**, 284 (1940).
2. E.K. Banghart, J.P. Lavine, J.M. Pimbley, and B.C. Burkey, COMPEL **1 0**, 205 (1991).
3. J.A. Cavaillès, D.A.B. Miller, J.E. Cunningham, P. Li Kam Wa, and A. Miller, Appl. Phys. Lett. **6 1**, 426 (1992).
4. N.G. van Kampen, Stochastic Processes in Physics and Chemistry (North-Holland, Amsterdam, 1981), Ch. 6.

5. Z. Schuss, Theory and Applications of Stochastic Differential Equations (John Wiley, New York, 1980), Ch. 8.
6. P. Hänggi, P. Talkner, and M. Borkovec, Rev. Mod. Phys. **6 2**, 251 (1990).
7. R.S. Larson and E.J. Lightfoot, Physica **1 4 9 A**, 296 (1988).
8. J.P. Lavine and B.C. Burkey, Solid-State Electronics **2 3**, 75 (1980).
9. J. P. Lavine, W.-C. Chang, C.N. Anagnostopoulos, B.C. Burkey, and E.T. Nelson, IEEE Trans. Electron Devices **E D - 3 2**, 2087 (1985).
10. Subroutines D02KAF and D02KDF from the NAG FORTRAN Library, Numerical Algorithms Group, Inc., Downers Grove, Illinois.
11. K.M. Hong and J. Noolandi, Surf. Sci. **7 5**, 561 (1978).
12. E. Parzen, Stochastic Processes (Holden-Day, San Francisco, 1962), Chs. 6 and 7.
13. N.S. Goel and N. Richter-Dyn, Stochastic Models in Biology (Academic Press, New York, 1974), Chs. 2 and 3 and the appendices.
14. D.T. Gillespie, Markov Processes: An Introduction for Physical Scientists (Academic Press, Boston, 1992), Chs. 3 and 6.
15. D.L. Weaver, Phys. Rev. B **2 0**, 2558 (1979).
16. D.L. Weaver, J. Chem. Phys. **7 2**, 3483 (1980).
17. J.M. Deutch, J. Chem. Phys. **7 3**, 4700 (1980).
18. G.H. Weiss, Adv. Chem. Phys. **1 3**, 1 (1967).
19. D.L. Weaver, Surf. Sci. **9 0**, 197 (1979).